Ultra-Stability and High Output Performance of Sliding Mode Triboelectric Nanogenerator Achieved by Asymmetric Electrode Structure Design

Gui Li,‡[a] Jian Wang,‡[b] Yue He,[c] Shuyan Xu,[b] Shaoke Fu,[b] Chuncai Shan,[b] Huiyuan Wu,[b] Shanshan An,[b] Kaixian Li,[b] Wen Li,[a] Ping Wang[a*] and Chenguo Hu[a, b*]

[a]*State Key Laboratory of Power Transmission Equipment Technology, School of Electrical Engineering, Chongqing University, Chongqing, 400044, P. R. China*

[b]*Department of Applied Physics, Chongqing University, Chongqing, 400044, P. R. China*

[c]*School of Geosciences and Info-Physics, Central South University, Changsha, 410083, P. R. China*

**E-mail: cqu_dqwp@cqu.edu.cn (P. W.), hucg@cqu.edu.cn (C. H.).*

‡ These authors contributed equally to this work.

Note 1. Charge distribution and calculation of AE-S-TENG.
Note 2. Charge accumulation process of AE-S-TENG.
Note 3. The different sliding states of AE-S-TENG and the corresponding output current.
Note 4. Charge accumulation process of AE-S-TENGs with the BLE area of 6 cm^2 (A1) and 9 cm^2 (A2).
Note 5. Charge accumulation process of the Model 1.
Note 6. Charge accumulation process of AE-S-TENG with TSE area of 12 cm^2 (B1).
Note 7. Charge accumulation process of rotation-AE-S-TENG.
Fig. S1. Photograph of AE-S-TENG and the corresponding electrodes size.
Fig. S2. Comparison of conventional S-TENG and AE-S-TENG moving equivalent distance.
Fig. S3. Initial charge distribution of AE-S-TENG.
Fig. S4. Output current of the AE-S-TENG working in different conditions.
Fig. S5. Charge increment process of AE-S-TENG.
Fig. S6. Output current of the AE-S-TENG working in different states.
Fig. S7. Output performance of AE-S-TENG with different BLE.
Fig. S8. Charge increment process of AE-S-TENG with the BLE area of 6 cm^2.
Fig. S9. Charge increment process of AE-S-TENG with the BLE area of 9 cm^2.
Fig. S10. Comparison of two models of AE-S-TENG.
Fig. S11. Charge increment process of AE-S-TENG with the BLE grounded. a) The 1st, b) 2nd, 3rd and d) (n+1)th process of charge transferring on the load.
Fig. S12. Charge increment process of AE-S-TENG with the TSE area of 12 cm^2.
Fig. S13. Output of AE-S-TENG loaded with different weights.
Fig. S14. Comparison of output current for AE-S-TENG with different tribo-pairs materials.
Fig. S15. Output performance of the AE-S-TENG working in different frequencies.

Fig. S16. Output voltage of the AE-S-TENG with various loads.
Fig. S17. The photograph of the rotor and the stator of rotation-type AE-S-TENG.
Fig. S18. Charge increment process of rotation-type AE-S-TENG.
Fig. S19. Output volatge of the rotation- AE-S-TENG under various impadence.
Fig. S20. Current curves of rotation-AE-S-TENG and correspondingly calculated RMS current under various impedance.
Fig. S21. The rotation-AE-S-TENG integrated with PMC
Video S1. 12 bulbs are powered by the rotation-AE-S-TENG.
Video S2. A buzzer is triggered by rotation-AE-S-TENG.
Video S3. 50 thermo-hygrometers are powered by the rotation AE-S-TENG.
Video S4. A mobile phone is powered by the rotation AE-S-TENG.

Note 1. Charge distribution and calculation of AE-S-TENG

In the initial state, the charge distribution of AE-S-TENG is illustrated in Fig. S4a. Here, Q_T and Q_p represent the charges on the BSE and PTFE, respectively, while Q_{L1} and Q_{R1} denote the charges on the PA. Furthermore, Q_{L1} and Q_{L2} represent the charges on the BLE and BSE, respectively. Given the electron affinity of different tribo-materials, an equal amount of negative and positive charges must be generated on the TENG at the initial contact state.

Therefore, we can derive that:

$$Q_T = Q_P + Q_{L1} + Q_{L2} \#(1)$$

$$Q_{R1} = -Q_{R2} \#(2)$$

Secondly, the charges on the AE-S-TENG are enable to further divide due to asymmetrical structure of the TENG, as shown in Fig. S4b. The corresponding equations is shown as follow:

$$Q_T = Q_1 \#(3)$$

$$Q_T = 2Q_0 \#(4)$$

$$Q_{L1} = 2Q_3 \#(5)$$

$$Q_{L1} = Q_2 + Q_4 \#(6)$$

$$Q_{R1} = -Q_{R2} = Q_3 \#(7)$$

According to Equation (1) and (2), the relationships of charges distribution are redefined as follow:

$$Q_0 = Q_3 + Q_4 \#(8)$$

$$Q_0 = Q_1 + Q_2 + Q_3 \#(9)$$

Besides, the top electrode and bottom electrode form two capacitors in parallel. Here, the voltage of capacitor 1 (U_1) and voltage of capacitor 2 (U_2) tend to be equal when AE-S-TENG reaches to equilibrium state.

$$U_1 = U_2 \#(10)$$

The capacitance equation and the relationship of charge, voltage and capacitance can be expressed as:

$$C = \frac{\varepsilon_r \varepsilon_0 S}{d} \#(11)$$

$$U = \frac{Q}{C} \#(12)$$

Where C is the capacitance of capacitor, ε_0 and ε_r are the permittivity of vacuum and relative permittivity of the dielectric film, respectively, S and d are the effective area electrodes and thickness of dielectric films, respectively.

According to Equation (10)-(12), we can obtain the relative charge in the overlapped electrodes area.

$$\frac{Q_1 d_1}{\varepsilon_{r1}\varepsilon_0 S} = \frac{Q_2 d_2}{\varepsilon_{r1}\varepsilon_0 S} \#(13)$$

Where ε_{r1} and ε_{r2} are the relative permittivity of PTEF and PA, d_1 and d_2 are the thickness of PTFE and PA, respectively. Here, in order to simplify the calculation, we suppose that $d_1/\varepsilon_{r1} = d_2/\varepsilon_{r2}$ and the charges on the PTFE is Q. Thus, the initial charges distribution is displayed in Fig. S4d and corresponding equations is given as follow:

$$Q_0 = -4Q \#(14)$$
$$Q_1 = Q_2 = Q \#(15)$$
$$Q_3 = Q_4 = 2Q \#(16)$$

This relationship is maintained in our subsequently theoretical analysis to simplify the theoretical analysis.

Note 2. Charge accumulation process of AE-S-TENG

Fig. 5 illustrates the entire process of triboelectrification and charge increment of AE-S-TENG. In this context, we define Q_{LMn}, Q_{MRn}, and Q_{tn} as the charges transferring on the load when the slider, after n cycles, moves from the left side to the middle position, the middle position to the right side, and the left side to the right side, respectively. When the slider initiates movement from the left side to the middle position, charge $3Q$ transfers from the BLE to the BSE. In this process, all charge passes through the load, as depicted in Fig. S5a (ii):

$$Q_{LM0} = 3Q \#(17)$$

When the slider subsequently moves from the middle position to the right sides, charge Q and $3Q$ transfer from the BLE to the BSE and the TSE, respectively (Fig. S5a (iii)). In this process, the charge Q_{MR0} passing through external load is express as:

$$Q_{MR0} = Q + 3Q = 4Q \#(18)$$

Thus, when the slider moves from the left side to the right side, the total charge Q_{t0} transferring on the load is the sum of Q_{LM0} and Q_{MR0}, as follows:

$$Q_{t0} = Q_{LM0} + Q_{MR0} = 7Q \#(19)$$

Meanwhile, as a result of triboelectrification between PTFE and PA, 2q charges are generated on the PA and accumulate in the blank area. Consequently, the charges on the PTFE covering the BSE increase to $-(4Q+2q)$. When the slider moves back from the right side to the middle position, charge Q and $3Q$ transfer back from the TSE and the BSE to the BLE, respectively. Simultaneously, the ground supplements q charges

to the BSE and the TSE to achieve electrostatic equilibrium (Fig. S5a (iv)). In this process, the reversed charge Q_{MR1} transferring on the load is expressed as:

$$Q_{MR1} = Q + 3Q = 4Q\#(20)$$

In the meantime, the *2q* charge on the surface of PA without the bottom electrode quickly dissipated. When the slider moves back to the left side, the charge Q_{LM1} transfers on the load, and the Q_{LM1} is expressed as (Fig. S5b (i)):

$$Q_{LM1} = 3Q + q\#(21)$$

Thus, the charge Q_{t1} reversely transfers on the external load from process (iii) to (v) and Q_{t1} is expressed as:

$$Q_{t1} = Q_{LM1} + Q_{MR1} = 7Q + q\#(22)$$

Therefore, the charge Q_{t1} is reversely transferred on the load when the slider moves from left to right again (Fig. S5b (i), (ii), and (iii)). Additional processes of charge transfer on the load are illustrated in Fig. S5b, c, and d. Based on the analysis and observations, we can conclude that the output charge will increase by the amount of charge *q* when AE-S-TENG operates for a cycle, and the transferring charges Q_{LMn} and Q_{MRn} after n cycles are expressed as (Fig. S5d):

$$Q_{LMn} = 3Q + nq\#(23)$$

$$Q_{MRn} = 4Q\#(24)$$

Thus, the Q_{tn} can be obtained, as follow:

$$Q_{tn} = Q_{LMn} + Q_{MRn} = 7Q + nq\#(25)$$

Note 3. Working mechanism of AE-S-TENG sliding in different states.

The transfer charge of the slider moving in the first half of the distance is illustrated in Fig. S6b. When the slider moves solely from the left side to the middle position, charge *3Q+nq* transfers from the BLE to the BSE (Fig. 6b(ii)). As the slider moves back to the left side, charges 3Q+nq reversely flow from the BSE to the BLE (Fig. 6b(i)). Consequently, the output charge depends on both the tribo-charge and accumulation charge when the slider moves the first half of the distance. The transfer charge of the slider moving in the second half of the distance is illustrated in Fig. S6c. Although there is the accumulation-charge generated on the PTFE, these charges (nq) only transfer between the BSE and the TSE, while charge 4Q transfers between the BLE and the BSE (Fig. S6c (i) and (ii)). Thus, only the tribo-charge transfers to the external load. Additionally, the transfer charge is associated with the moving distance (larger distance generates a larger transfer charge). Therefore, the output charge when the slider moves the entire distance is larger than the superposition of the output charge when the slider moves the first half of the distance and the second half of the distance.

Note 4. Charge accumulation process of AE-S-TENG with the BLE area of 6 cm^2 (A1) and 9 cm^2 (A2)

Fig. S8 illustrates the entire process of triboelectrification and charge increment of AE-S-TENG with a BLE of 6 cm2 (A1). In the initial state, the charge distribution of the TENG is displayed in Fig. S8a (i). As the slider starts moving from the left side to the middle position, charge *Q* and *3Q* transfer from the ground to the BLE and the BSE, respectively (Fig. S8a (ii)). In this process, the external load experiences a reverse

charge Q_{LM0} transferring, as follows:

$$Q_{LM0} = -Q \#(26)$$

When the slider subsequently moves to the right side, the charge transferring on the load is the same as the process from Fig. S5a (ii) to Fig. S5a (iii), as shown in Fig. S8a(iii). Hence, the charge Q_{MR0} passing through the external load is expressed as:

$$Q_{MR0} = Q + 3Q = 4Q \#(27)$$

Thus, when the slider moves from the left side to the right side, the total charge Q_{t0} transferring on the load is:

$$Q_{t0} = Q_{LM0} + Q_{MR0} = 3Q \#(28)$$

Meanwhile, the $2q$ charges generate on the PA satiated in the blank area on the right side, and the charges on the PTFE covered on the BSE increase to $-(4Q+2q)$. When the slider moves back from the right side to the middle position, the charge transferring on the load is the same as the process from Fig. S5a (iii) to Fig. S5a (iv), as shown in Fig. S8a (iv). Thus, the reversed charge Q_{MR1} transferring on the load is expressed as:

$$Q_{MR1} = Q + 3Q = 4Q \#(29)$$

When the slider subsequently moves to the left position, charge $2Q$ transfers from BLE to the ground, and charge $Q+q$ transfers from the BSE to the BLE (Fig. S8b (i)). Additionally, the $4Q+2q$ charges generate on the PA saturated in the blank area on the left side, and the charges on the PTFE covered on the BSE increase to $-(4Q+2q)$. The charge Q_{LM1} transferring on the load is expressed as (Fig. S8b (i)):

$$Q_{LM1} = Q + q - 2Q = q - Q \#(30)$$

Thus, the charge Q_{t1} reversely transfers on the external load from process Fig.S8a (iii) to b(i) and Q_{t1} is expressed as:

$$Q_{t1} = Q_{LM1} + Q_{MR1} = 3Q + q \#(31)$$

When the slider moves again from the left side to the middle position, charges $Q+q$ and $2Q$ transfer from the ground to the BSE and the BLE, respectively (Fig. S8b (ii)). Meanwhile, the $4Q+2q$ charge on the surface of PA without the bottom electrode quickly dissipates, and the q charges transfer from the ground to BLE to balance the potential difference. In this process, the external load experiences charge transferring, as follows:

$$Q_{LM1} = -Q + q - q = -Q \#(32)$$

When the slider subsequently moves from the middle position to the right side, charge $Q+q$ and $3Q$ transfer from the BLE to the BSE and the TSE, respectively (Fig. S8b (iii)). In this process, the charge Q_{MR1} passing through the external load is expressed as:

$$Q_{MR1} = Q + q + 3Q = 4Q + q \#(33)$$

Thus, the charge Q_{t1} transfers on the external load from process Fig S8 b (i) to b (iii) and Q_{t1} is expressed as:

$$Q_{t1} = Q_{LM1} + Q_{MR1} = 3Q + q \#(34)$$

More processes of transfer charge on the load are shown in Fig. S8b, c and d. The output charge will increase the amount of charge q when AE-S-TENG operates a period and the transferring charge Q_{LMn} and Q_{MRn} after n cycles is expressed as (Fig. S8d):

$$Q_{LRn} = -(Q + nq - nq) = Q \#(35)$$

$$Q_{MRn} = 4Q + nq \#(36)$$

Thus, the Q_{tn} can be obtained, as follows:

$$Q_{tn} = Q_{LMn} + Q_{MRn} = 3Q + nq\#(37)$$

Additionally, Fig. S9 illustrates the entire process of triboelectrification and charge increment of AE-S-TENG with a BLE of 9 cm^2 (A2). Considering the bottom blank area on the left, the charge distribution is further subdivided. Hence, the charge distribution in the initial state is displayed in Fig. S9 (i). As the slider starts moving from the left side to the middle position, charge Q and $2Q$ transfer from the BLE and the ground to the BSE, respectively (Fig. S9a (ii)). In this process, there is charge Q transferring on the load, as follows:

$$Q_{LM0} = Q\#(38)$$

When the slider subsequently moves to the right side, the charge transferring on the load is the same as the process from Fig. S5a (ii) to Fig. S5a (iii), as shown in Fig. S9a (iii). Hence, the charge Q_{MR0} passing through the external load is expressed as:

$$Q_{MR0} = Q + 3Q = 4Q\#(39)$$

Thus, when the slider moves from the left side to right side, the total charge Q_{t0} transferring on the load is:

$$Q_{t0} = Q_{LM0} + Q_{MR0} = 5Q\#(40)$$

Meanwhile, the $2q$ charges generate on the PA saturated in the blank area, and the charges on the PTFE covered on the BSE increase to $-(4Q+2q)$. When the slider moves back from the right side to the middle position, charge transferring on the load is also the same as the process from Fig. S5a (iii) to Fig. S5a (iv), as shown in Fig. S9a (iv). Thus, the reversed charge Q_{MR1} transferring on the load is expressed as:

$$Q_{MR1} = Q + 3Q = 4Q\#(41)$$

When the slider subsequently moves to the left position, charges $Q+q$ and $2Q$ transfer from the BSE to the BLE and the BSE to the ground, respectively. Thus, the charge Q_{LM1} transferring on the load is expressed as (Fig. S9b (i)):

$$Q_{LM1} = Q + q\#(42)$$

Meanwhile, the q charges generated on the PA satiated in the blank area on the left side, and the charges on the PTFE covering the BSE increase to $-(2Q+2Q+q=4Q+q)$. Consequently, the charge Q_{t1} undergoes reverse transfer to the external load from the process depicted in Fig. S9a (iii) to b(i), and Q_{t1} is expressed as:

$$Q_{t1} = Q_{LM1} + Q_{MR1} = 5Q + q\#(43)$$

When the slider moves from the left side back to the middle position, charge $Q+q$ transfers from BLE and BSE, respectively (Fig. S8b (ii)). Simultaneously, the $2Q+q$ charge on the surface of PA without the bottom electrode quickly dissipates, and the q charge transfers from the ground to BLE to balance the potential difference. In this process, there is charge transfer in the external load, as follows:

$$Q_{LM1} = Q + q - q = Q\#(44)$$

When the slider subsequently moves from the middle position to the right sides, charge $Q+q$ and $3Q$ transfer from the BLE to the BSE and the TSE, respectively (Fig. S9b (iii)). In this process, the charge Q_{MR1} passing through external load is express as:

$$Q_{MR1} = Q + q + 3Q = 4Q + q\#(45)$$

Thus, the charge Q_{t1} transfers on the external load from process b (iii) to b (iv) and Q_{t1} is expressed as:

$$Q_{t1} = Q_{LM1} + Q_{MR1} = 5Q + q\#(46)$$

More processes of transfer charge on the load are shown in Fig. S8b, c and d. Thus, the output charge will increase the amount of charge q when AE-S-TENG operates a period and the transferring charge Q_{LMn} and Q_{MRn} after n cycles is expressed as (Fig. S9d):

$$Q_{LMn} = Q \#(47)$$

$$Q_{MRn} = 4Q + nq \#(48)$$

Thus, the Q_{tn} can be obtained, as follow:

$$Q_{tn} = Q_{LMn} + Q_{MRn} = 5Q + nq \#(49)$$

From Equations (25), (37), and (49), we can theoretically conclude that the output charge increases with the increment of the area of BLE when the AE-S-TENG slides the same distance, and the area of BLE influences the tribo-charge.

Note 5. Charge accumulation process of Mode 1

Fig. S11 illustrates the entire process of charge increment for Mode 1. During the charge increment process, the charge on the surface of PTFE and electrodes is the same as Mode 2 (Fig. S5). However, there is a noticeable difference in the charge transfer on the external load. To simplify the analysis process, the charge transfer on the load after n working cycles is used for analysis. When the slider moves from the left side to the middle position, charge $3Q+nq$ transfers from the BLE to the BSE (from Fig. 11d (i) to Fig. 11d (ii)). Thus, in this process, the charge Q_{LMn} passing through the load is:

$$Q_{LMn} = 3Q + nq \#(50)$$

When the slider subsequently moves to the right sides, charge Q and nq transfer from the BLE to BSE and from the BSE to the TSE, respectively (Fig. S11d (iii)). Thus, in this process, charge Q_{MRn} passing on the load is:

$$Q_{MRn} = Q - nq \#(51)$$

Thus, the total charge Q_{tn} transferring on the load is:

$$Q_{tn} = Q_{LMn} + Q_{MRn} = 4Q \#(52)$$

In Mode 1, the whole process of transfer charge is only related to tribo-charge. Therefore, Mode 2 demonstrates superior output performance compared to Mode 1.

Note 6. Charge accumulation process of AE-S-TENG with TSE area of 12 cm^2 (B2)

Fig. S12 shows the whole process of charge increment of B2 in Fig. 2i. The initial charge distribution is presented in Fig. S12a (i). As the slider moves from the left side to the middle position, $3Q$ charge transfers from the BLE to the BSE, resulting in a charge of Q_{LM0} (Fig. S12a (ii)):

$$Q_{LM0} = 3Q \#(53)$$

As the slider progresses from the middle position to the right side, a charge of $3Q$ is transferred from the BLE to the TSE. The resulting charge passing through the external load is denoted as Q_{MR0} (Fig. S12a (iii)):

$$Q_{MR0} = 3Q \#(54)$$

Therefore, as the slider moves from the left side to the right side, the total transferred charge on the load, denoted as Q_{t0}, is:

$$Q_{t0} = Q_{LM0} + Q_{MR0} = 6Q \#(55)$$

Meanwhile, charges on the PTFE covering the BSE increase to $-(4Q+2q)$ due to triboelectrification between PA satiated in the blank area and the PTFE. When the slider

moves back from the right side to the middle position, a reverse transfer of charge *3Q* occurs from the TSE to the BLE. Additionally, the ground replenishes a charge to both TSE and BSE to achieve electrostatic equilibrium (Fig. S12a (iv)). Thus, the reversed charge, denoted as Q_{MR1}, transferred on the load is expressed as:

$$Q_{MR1} = 3Q \#(56)$$

When the slider subsequently moves to the left position, a charge of *3Q+q* transfers from the BSE to the BLE. And the transferred charge Q_{LM1} on the load is expressed as (Fig. S12b (i)):

$$Q_{LM1} = 3Q + q \#(57)$$

Consequently, the charge Q_{t1} reversely transfers on the external load from process (iii) to (iv) and Q_{t1} is expressed as:

$$Q_{t1} = Q_{LM1} + Q_{MR1} = 6Q + q \#(58)$$

Therefore, the charge Q_{LR1} is reversely transferred on the load when the slider moves from left to right again (Fig. S12b (i), (ii) and (iii)). More processes of transfer charge on the load are shown in Fig. S12b, c and d. The output charge will increase the amount of charge q when AE-S-TENG operates a period and the transferring charge Q_{LMn}, Q_{MRn}, and the total charge Q_{tn} after n cycles is expressed as (Fig. S5d):

$$Q_{LMn} = 3Q + nq \#(59)$$

$$Q_{LMn} = 3Q + nq \#(60)$$

$$Q_{tn} = Q_{LMn} + Q_{MRn} = 6Q + nq \#(61)$$

Compared with Equation (25), we can make theoretically conclusion that output charge increases with decrement of the area of TSE when the AE-S-TENG slides same distance, and the area of TSE also influence the tribo-charge.

Note 7. Charge accumulation process of rotation-AE-S-TENG

Fig. S11 illustrates the complete process of charge increment for the rotation-AE-S-TENG. As a unit of the rotor rotates from the left side to the right side, the charge transfer mirrors the process depicted in Fig. S5a(i) to Fig. S5a(iii), as demonstrated in Fig. S8a(iii) and Fig.12a (i), (ii), and (iii). Consequently, there is a transfer of 7Q charges on the load. Simultaneously, the charge on the PTFE covering the BSE increases to *–(4Q+2q)*. However, as the rotor subsequently rotates to the right side, the total charges on the PTFE surface reach *-(8Q+4q)* due to the interaction between the PTFE in the blank area and the PA in the blank area, as illustrated in Fig. S12a(iv). Meanwhile, half of the next unit of the AE-S-TENG moves to the top of BLE. As a result, charge *3Q* transfers from the TSE to the BLE, and the ground replenishes charge q to the BLE and TSE, respectively. In this process, the reversed charge Q_{LM1} transferred on the load is:

$$Q_{LM1} = 3Q + q \#(62)$$

When the next unit subsequently rotates to the right side, as shown in S12b (i), Charge Q_{MR1} transfers from the ground to BLE to achieve a new electrostatic equilibrium, and the Q_{MR1} is:

$$Q_{MR1} = 4Q + 2q \#(63)$$

Thus, the charge Q_{t1} reversely transfers on the external load is (From Fig. S12 a(iii) to Fig. S12b (i)):

$Q_{t1} = Q_{LM1} + Q_{MR1} = 7Q + 3q\#(64)$

Subsequently, the charge Q_{tl} is reversely transferred on the load again when the unit continuously rotates to the right side (from Fig. S12b (i) to Fig. S12b (i)). Additional processes of charge transfer onto the load are depicted in Fig. S12b, c, and d. Based on the above analysis and observation, it can be concluded that the output charge will increment by the amount of charge *3q* when the rotation-type AE-S-TENG operates for a cycle, and the transferred charges Q_{LMn} and Q_{MRn} after n cycles are expressed as (Fig. S5d):

$Q_{LRn} = 3Q + nq\#(65)$

$Q_{MRn} = 4Q + 2nq\#(66)$

Thus, the Q_{tn} can be obtained, as follow:

$Q_{tn} = Q_{LMn} + Q_{MRn} = 7Q + 3nq\#(67)$

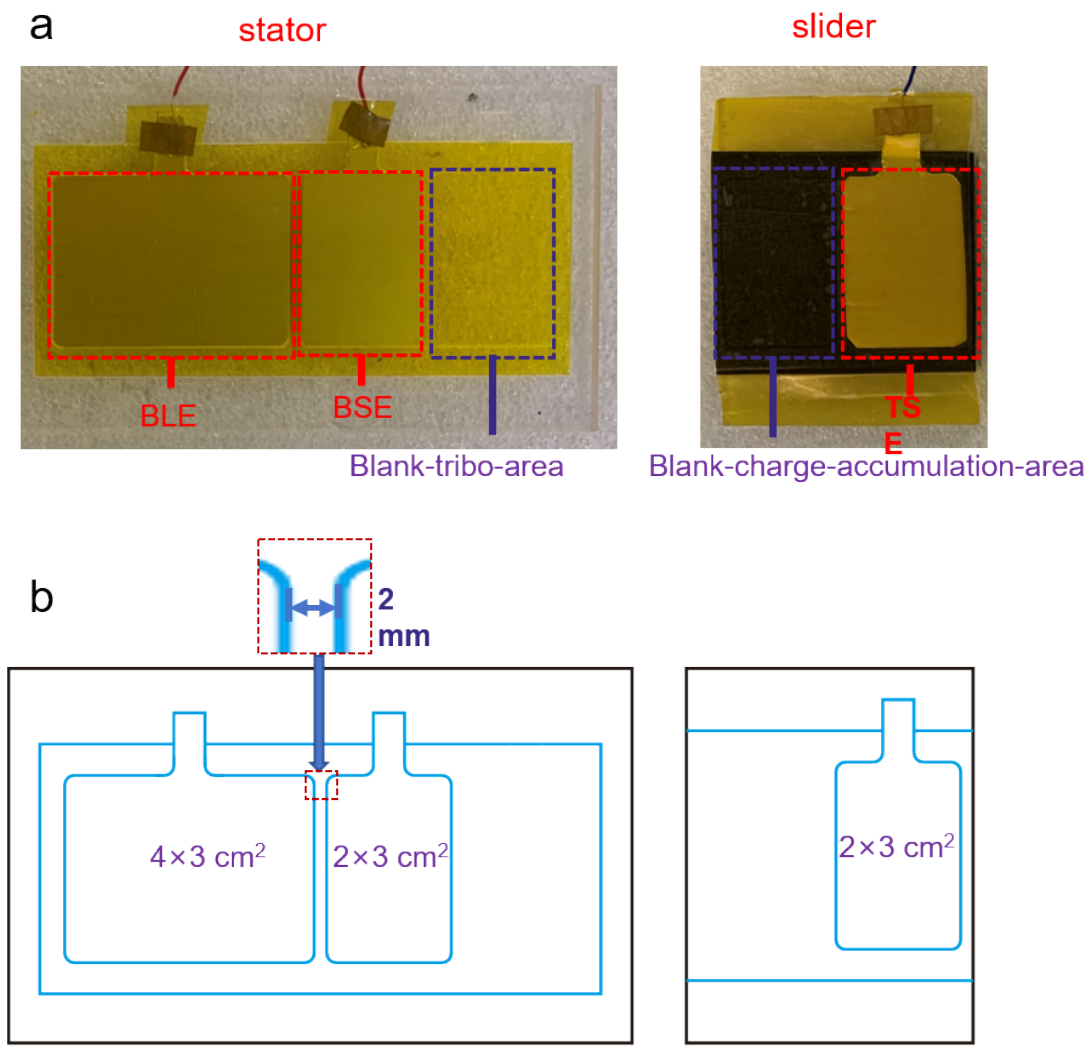

Fig. S1. a) Photograph of AE-S-TENG and b) the corresponding electrodes size.

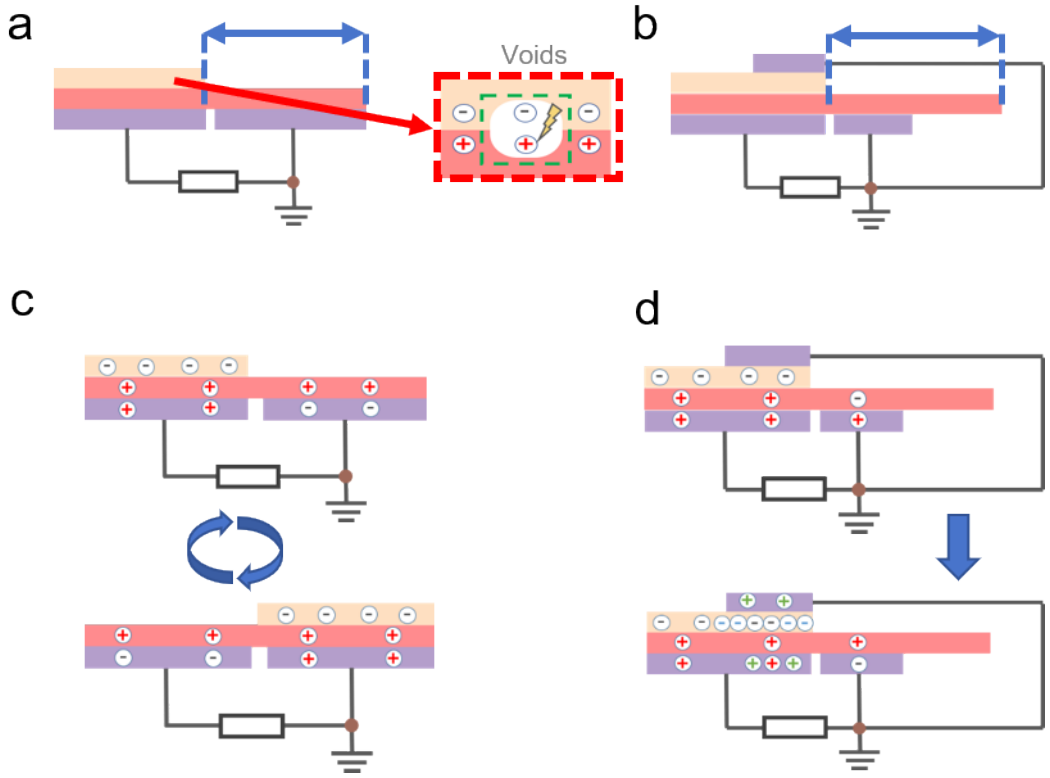

Fig. S2. Comparison of conventional S-TENG and AE-S-TENG. a) Conventional S-TENG and b) AE-S-TENG moving equivalent distance. c) Working mechanism of the S-TENG. d) Charge increment diagram of AE-S-TENG.

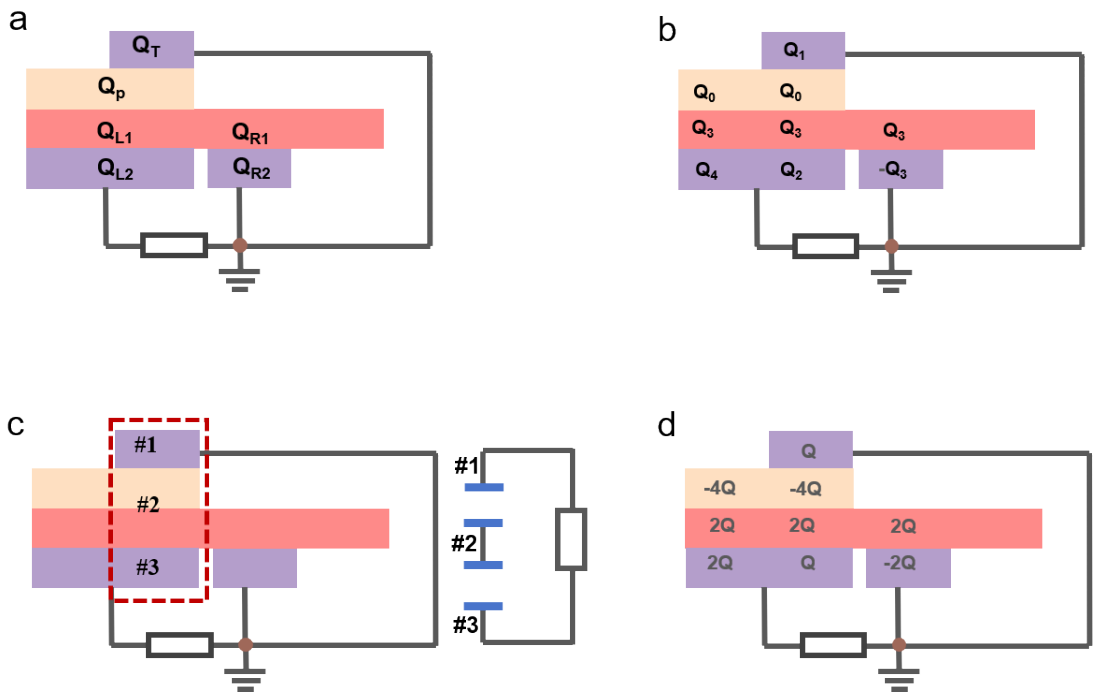

Fig. S3. Initial charge distribution of AE-S-TENG. a) Total charge quantity of each part. b) Redefined charge distribution of the AE-S-TENG. c) Equivalent capacitance of the AE-S-TENG. d) The final simplified charge distribution of the AE-S-TENG.

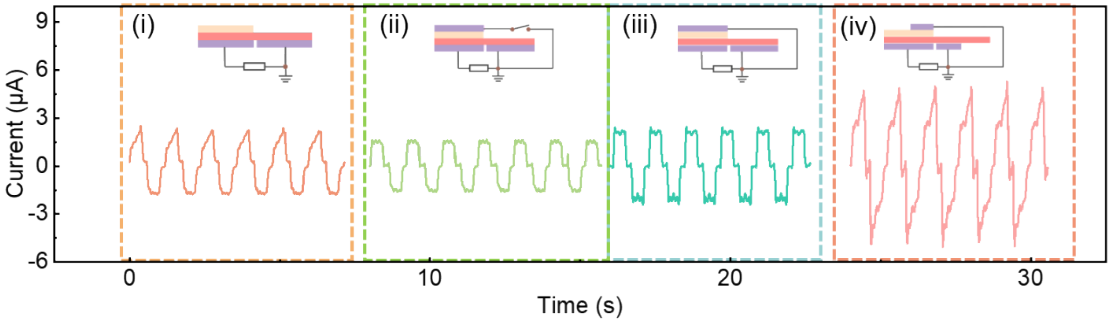

Fig. S4. Output current of the AE-S-TENG working in different conditions.

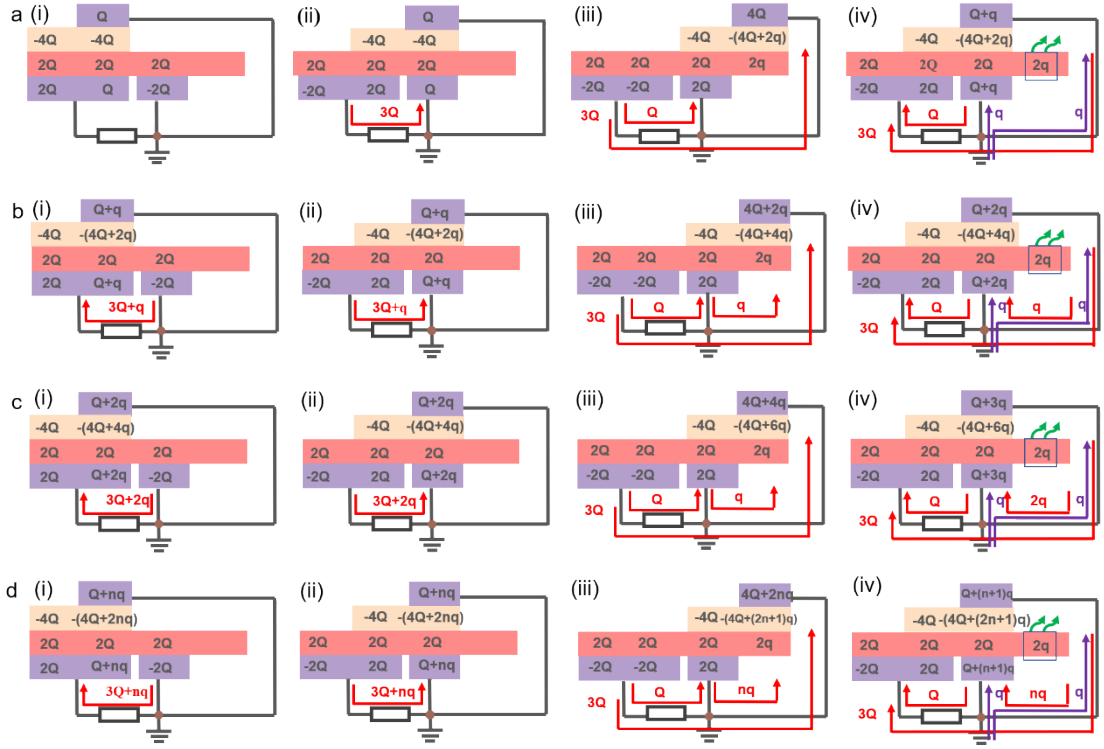

Fig. S5. Charge increment process of AE-S-TENG. a) The 1st, b) 2nd, 3rd and d) (n+1)th process of charge transferring on the load.

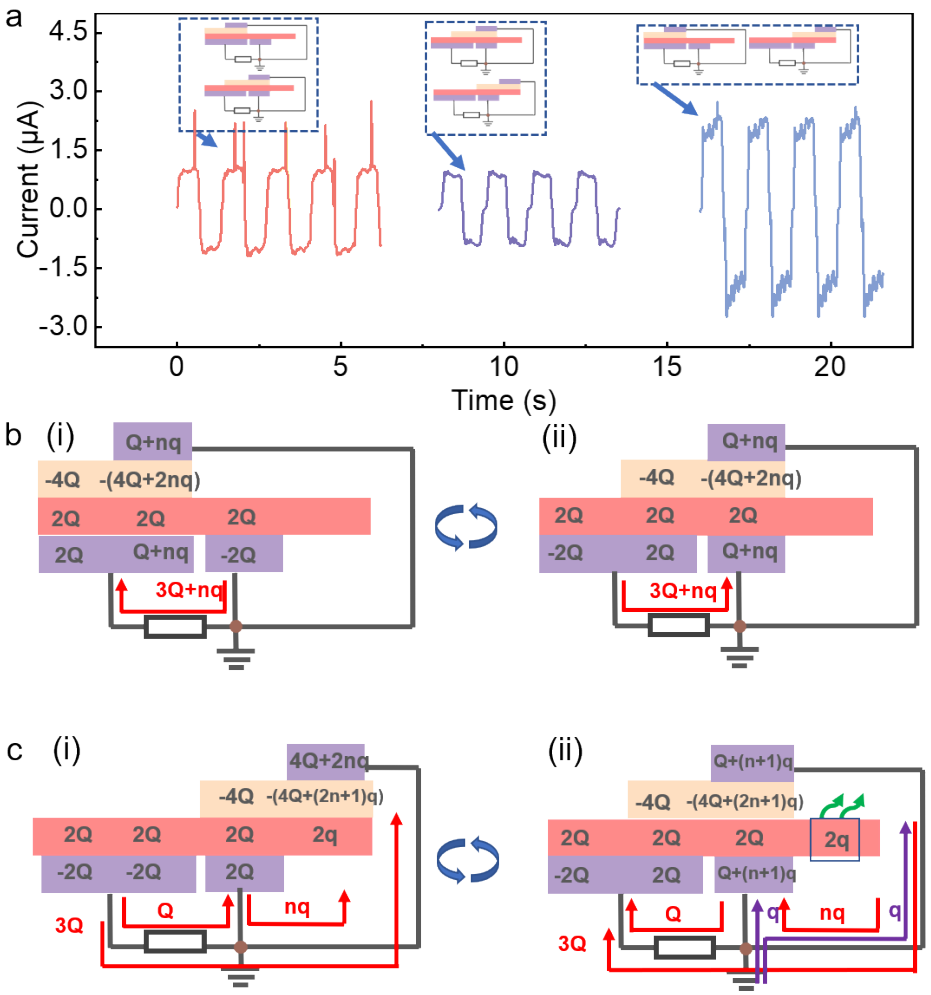

Fig S6. The different sliding states of AE-S-TENG and the corresponding output current. a) The output current of the AE-S-TENG works in different conditions. Charge transfer process of AE-S-TENG b) in the first half the distance and c) the second half the distance.

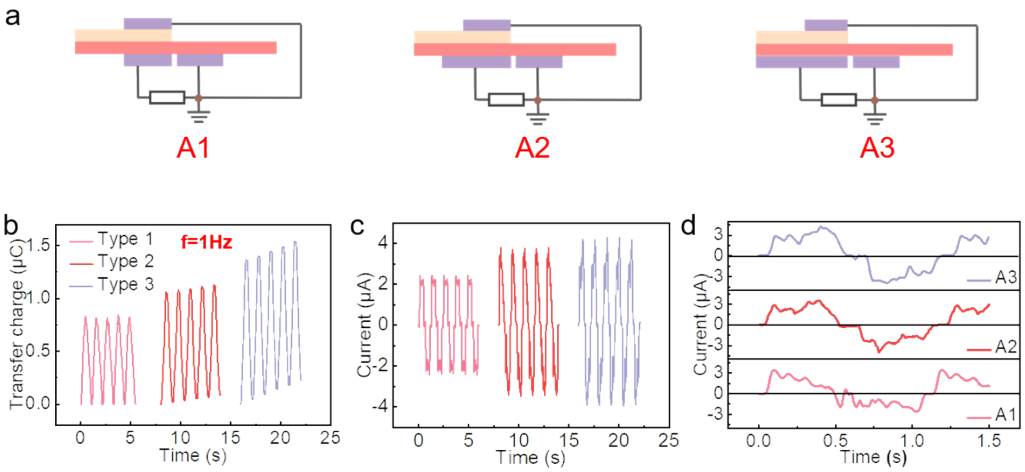

Fig. S7. Output performance of AE-S-TENG with different BLE. a) Cross-section of 3 types of the AE-S-TENG. b) Output charge, c) current and d) corresponding current curves of 3 types of the TENG.

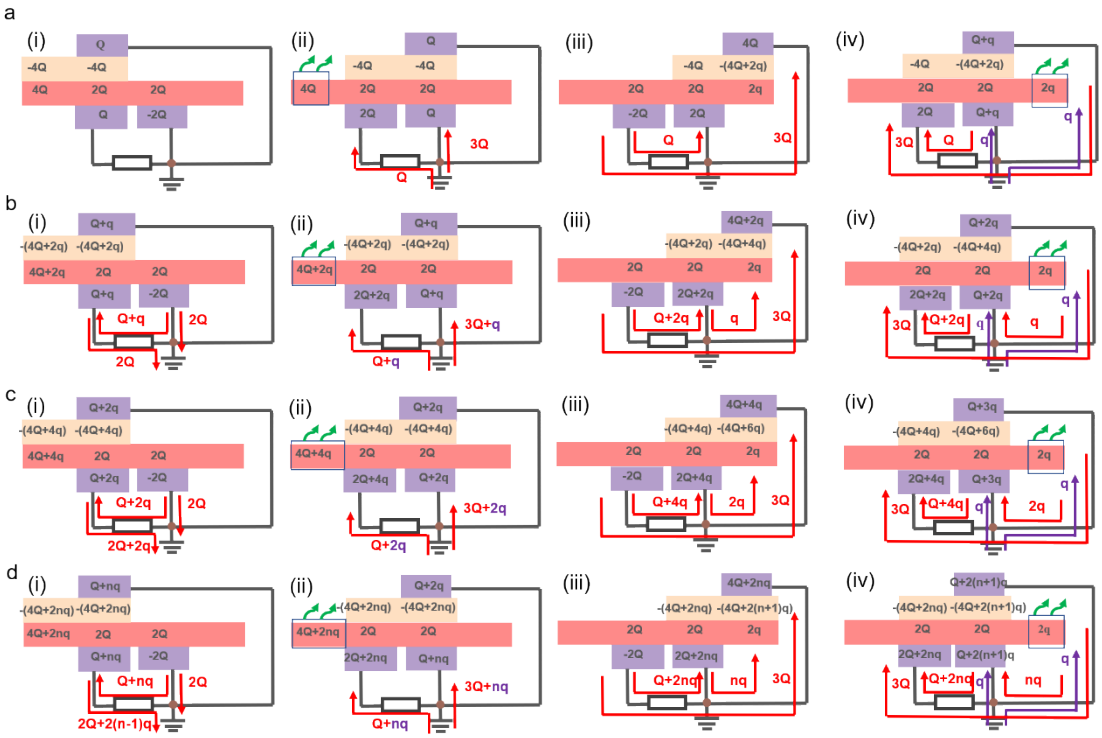

Fig. S8. Charge increment process of AE-S-TENG with the BLE area of 6 cm^2 (A1). a) The 1st, b) 2nd, 3rd and d) (n+1)th process of charge transferring on the load.

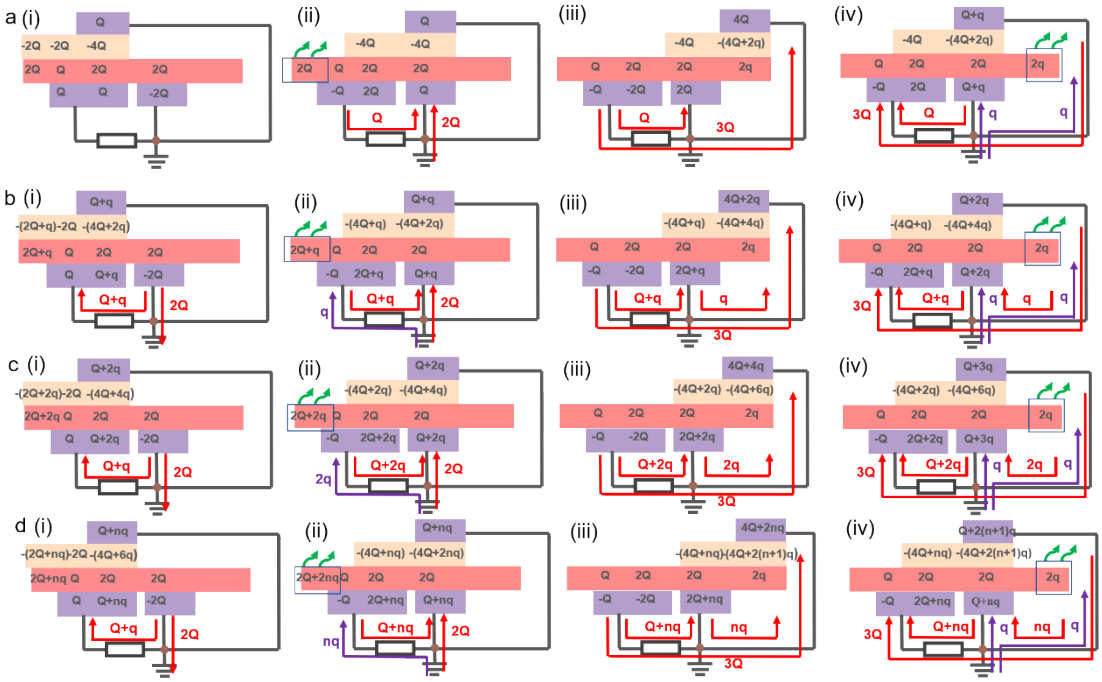

Fig. S9. Charge increment process of AE-S-TENG with the BLE area of 9 cm^2 (A1). a) The 1st, b) 2nd, 3rd and d) (n+1)th process of charge transferring on the load.

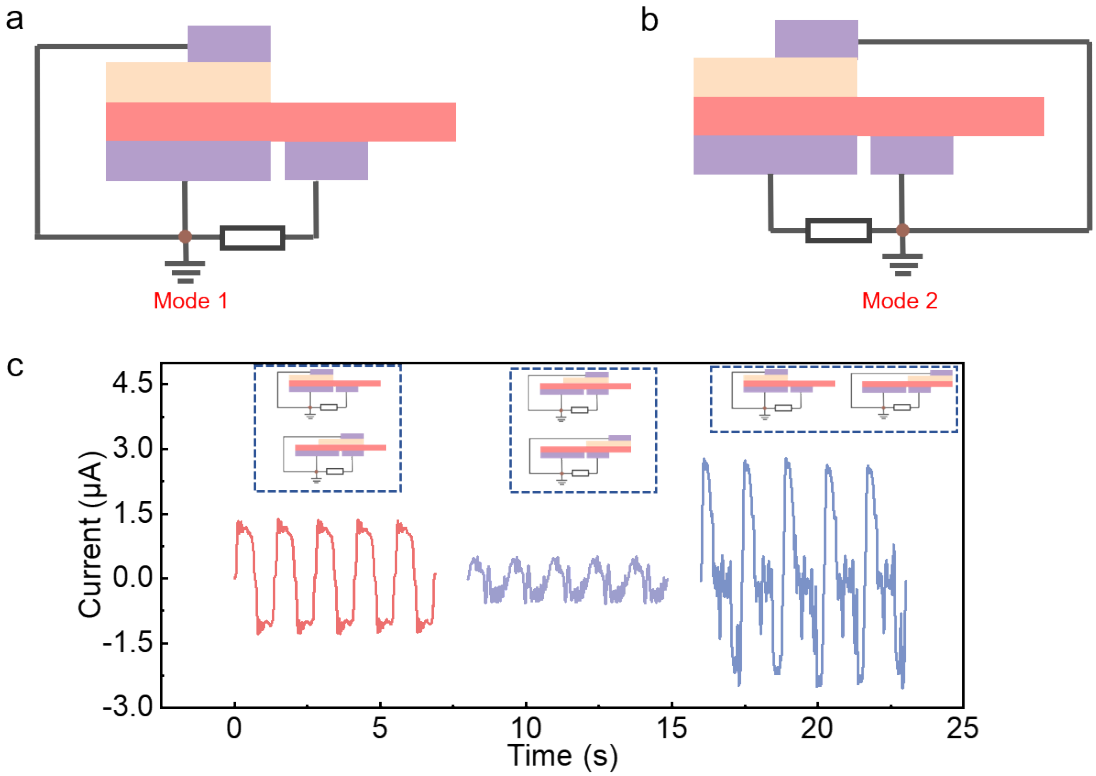

Fig. S10. Comparison of two models of AE-S-TENG. a) The BLE grounded. b) The BSE grounded. c) Output current of the Model 1 working in different conditions.

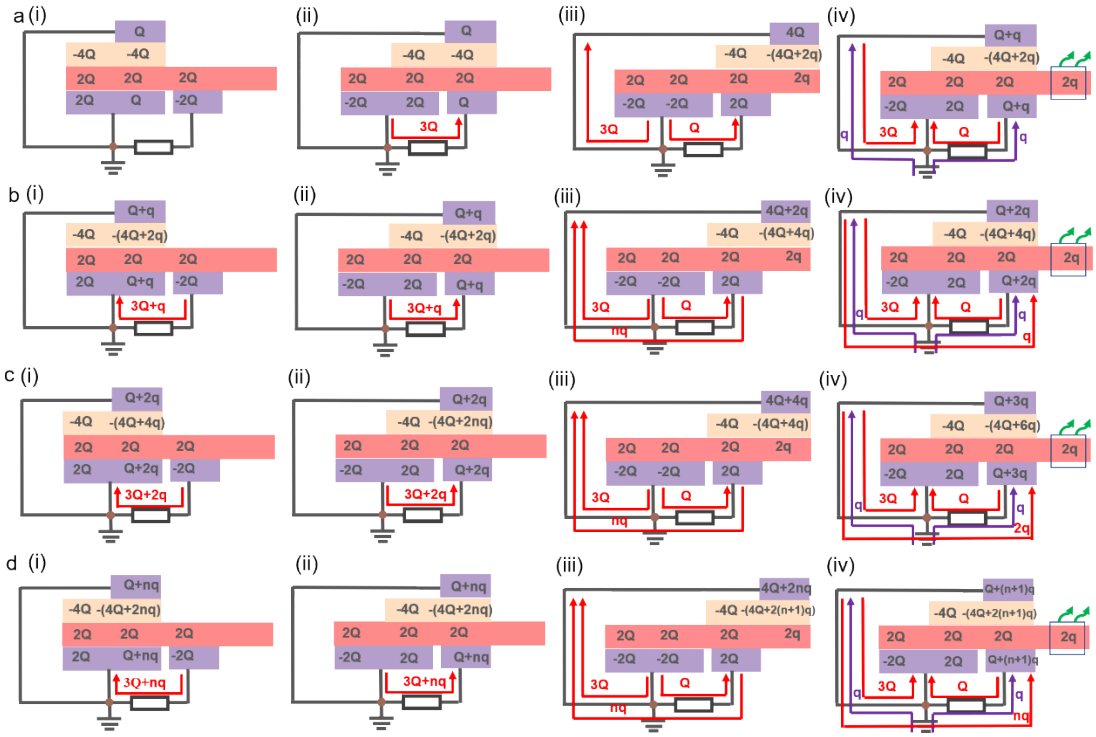

Fig. S11. Charge increment process of AE-S-TENG with the BLE grounded. a) The 1st, b) 2nd, 3rd and d) (n+1)th process of charge transferring on the load.

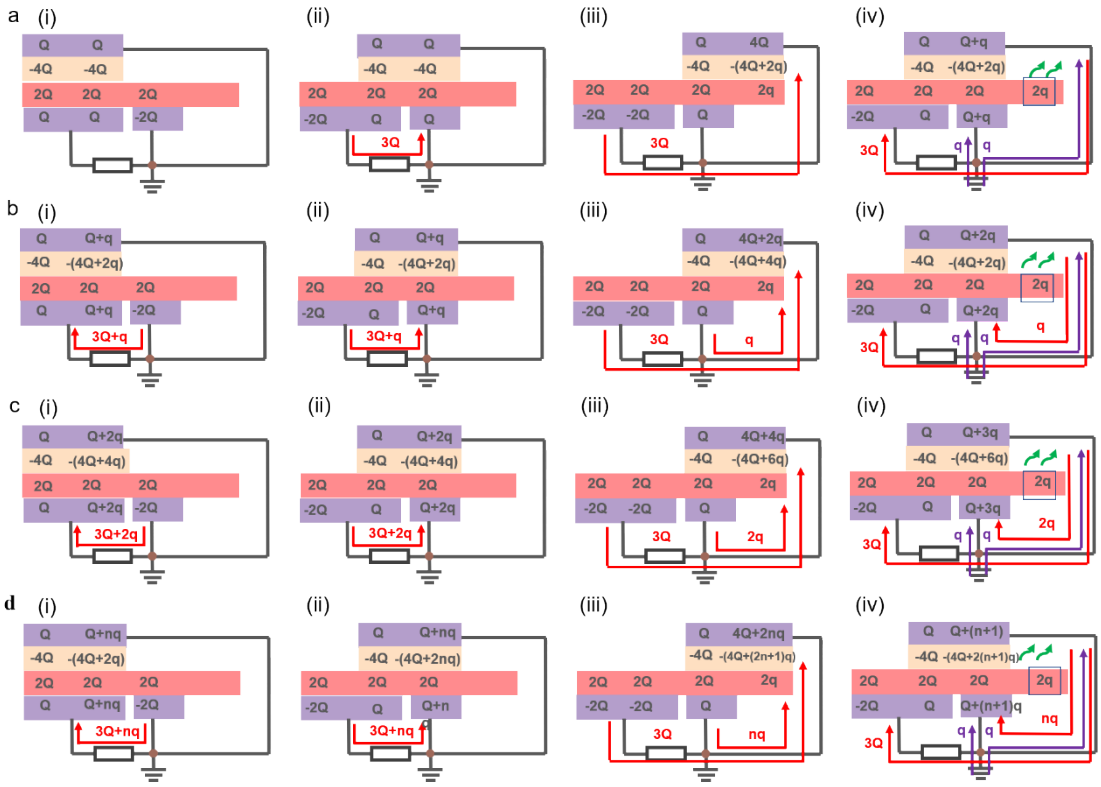

Fig. S12. Charge increment process of AE-S-TENG with the TSE area of 12 cm^2. a) The 1st, b) 2nd, 3rd and d) (n+1)th process of charge transferring on the load.

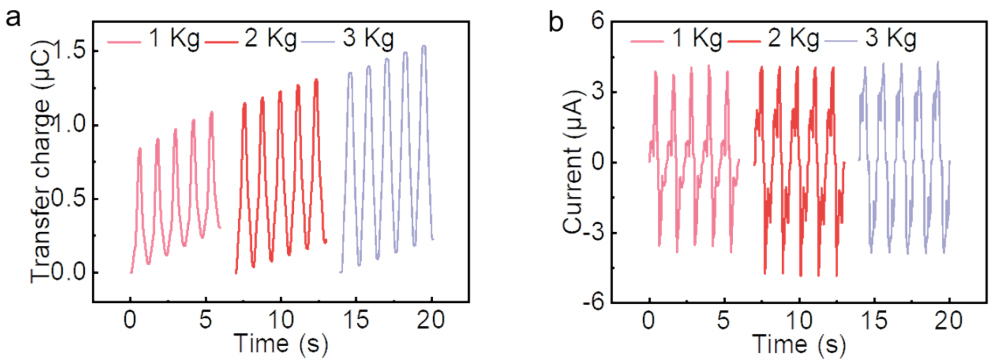

Fig. S13. Output of AE-S-TENG loaded with different weights. a) The corresponding output charge and b) current curves.

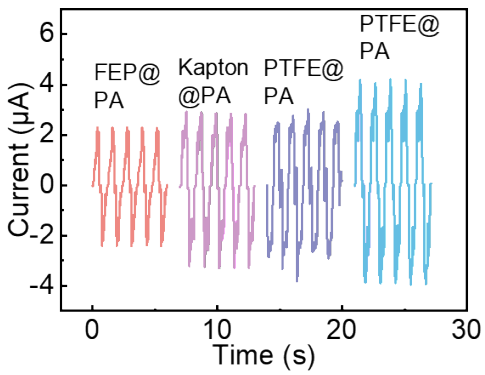

Fig. S14. Comparison of output current for AE-S-TENG with different tribo-pairs materials.

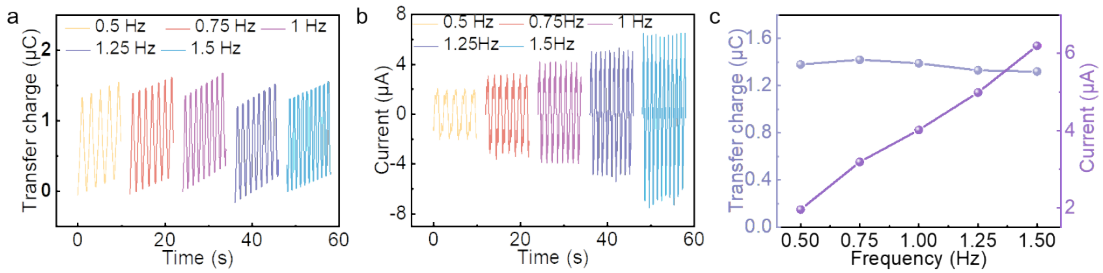

Fig. S15. Output performance of the AE-S-TENG working in different frequency. a) The corresponding a)charge and b) current curves.

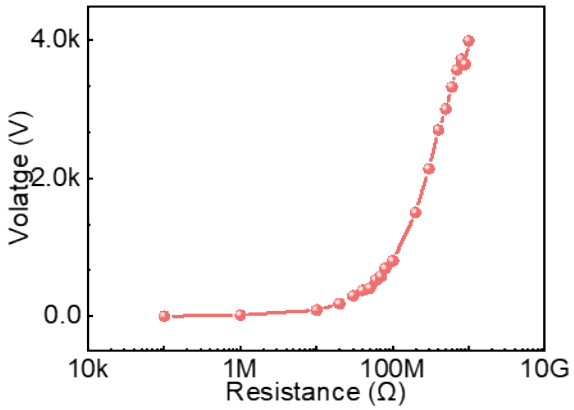

Fig. S16. Output voltage of the AE-S-TENG with various loads.

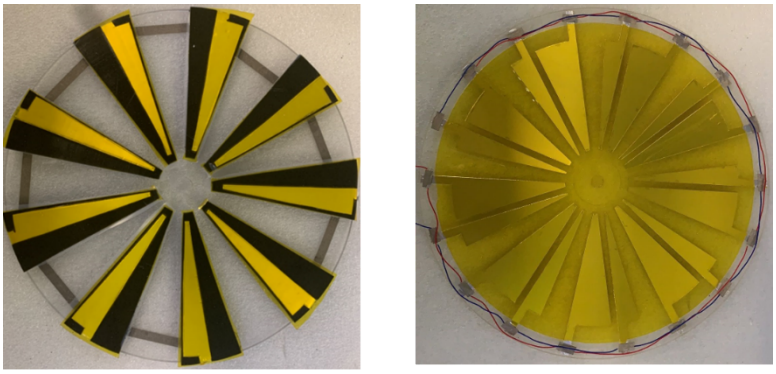

Fig. S17. The photograph of the rotor and the stator of rotation-type AE-S-TENG.

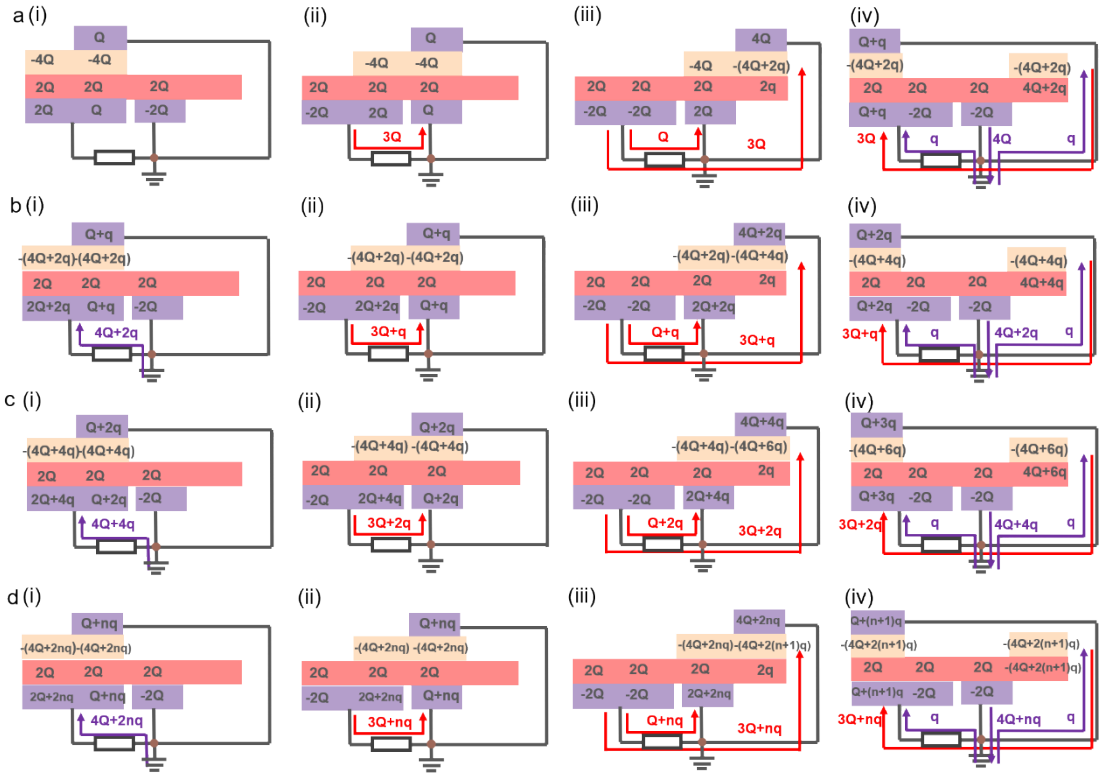

Fig. S18. Charge increment process of rotation-AE-S-TENG. a) The 1st, b) 2nd, 3rd and d) (n+1)th process of charge transferring on the load.

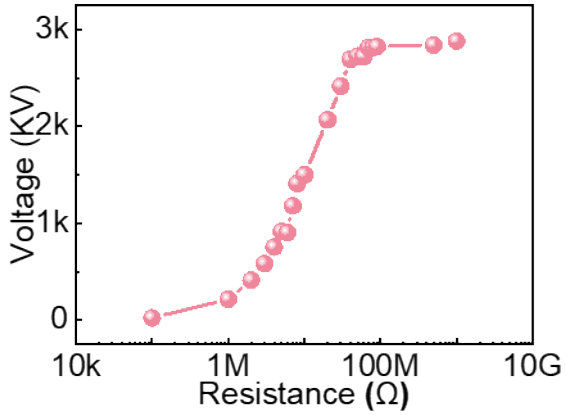

Fig. 19. Output volatge of the rotation-type AE-S-TENG under various impadence.

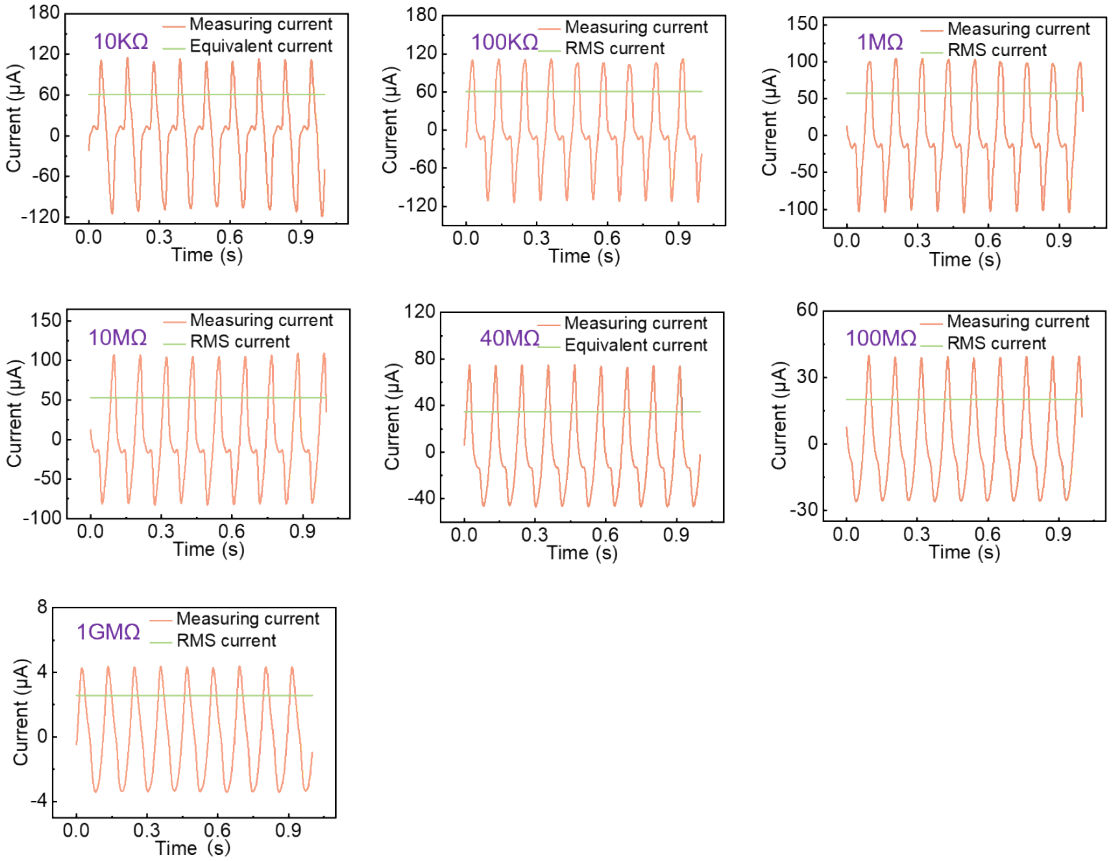

Fig. S20. Current curves of rotation-type AE-S-TENG and correspondingly calculated RMS current under various impedance.

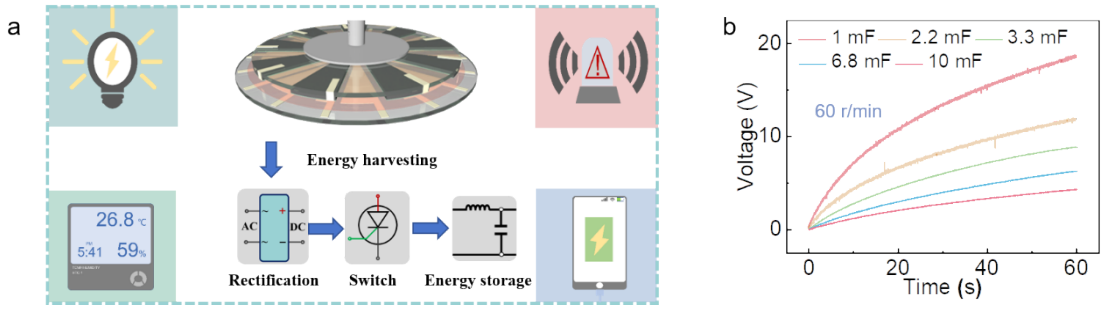

Fig. S21. The rotation-AE-S-TENG integrated with PMC. a) Framework diagram of the rotation-AE-S-TENG integrated with PMC for power supply. b) Various large capacitors charged by the AE-S-TENG with a PMC at 60 rpm.